

Intramolecular Ferromagnetic Radical–Cu<sup>II</sup> Coupling in a Cu<sup>II</sup> Complex Ligated with Pyridyl-Substituted Triarylmethyl Radicals

Tetsuro Kusamoto,\* Yohei Hattori, Akira Tanushi, and Hiroshi Nishihara\*

Department of Chemistry, Graduate School of Science, The University of Tokyo, 7-3-1 Hongo, Bunkyo-ku, Tokyo 113-0033, Japan

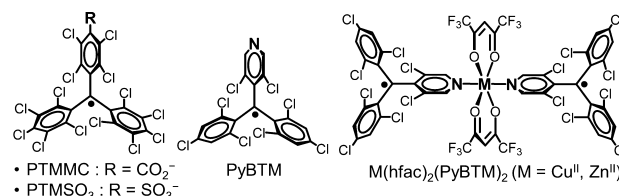
## Supporting Information

**ABSTRACT:** Novel metal complexes M-(hfac)<sub>2</sub>(PyBTM)<sub>2</sub> [M = Cu<sup>II</sup>, Zn<sup>II</sup>; hfac = hexafluoroacetylacetonato; PyBTM = (3,5-dichloro-4-pyridyl)bis(2,4,6-trichlorophenyl)methyl radical] were prepared. Both hexacoordinated complexes had elongated octahedral geometry, in which two PyBTM molecules coordinated at the equatorial positions in Cu<sup>II</sup>(hfac)<sub>2</sub>(PyBTM)<sub>2</sub> but at the axial positions in Zn<sup>II</sup>(hfac)<sub>2</sub>(PyBTM)<sub>2</sub>. Magnetic studies revealed an intramolecular ferromagnetic exchange interaction between the spins on PyBTM and Cu<sup>II</sup> ( $J_{\text{Cu-R}}/k_{\text{B}} = 47$  K) based on the orthogonality of the two spin orbitals.

Open-shell radicals have been extensively studied in recent decades as potential components of functional molecular materials because of their magnetic, electron-conducting, optical, and redox properties.<sup>1</sup> In particular, combining organic radicals with paramagnetic transition-metal ions is a promising strategy to yield unusual magnetic systems based on radical–metal exchange interactions. Such systems include single-chain magnets,<sup>1b</sup> light-responsive breathing crystals,<sup>1c</sup> and stepwise neutral-to-ionic transitions with a sensitive magnetic response.<sup>1d</sup> To achieve these magnetic characteristics, it is important to understand key factors that dominate the magnetic interaction. A radical–metal magnetic interaction is often rationalized by the overlapping or orthogonality of two spin orbitals (one each from the radical and metal ion), which mediates antiferromagnetic (AFM) or ferromagnetic (FM) interactions, respectively. The coordination geometry of a radical ligand at a metal center affects the strength ( $J$ , an exchange constant) and sign (FM or AFM) of a through-bond radical–metal interaction because the geometry defines whether the spin orbitals are overlapping or orthogonal.<sup>2</sup>

Polychlorinated triphenylmethyl radicals (PTMs) have attracted much attention as useful components of functional electronic devices,<sup>3</sup> although only a small variety of magnetic metal complexes with PTM ligands have been reported. Veciana and co-workers prepared a Cu<sup>II</sup> complex coordinated with two monocarboxylic PTMs (PTMCMs in Chart 1), [Cu<sup>II</sup>(PTMCM)<sub>2</sub>(H<sub>2</sub>O)<sub>3</sub>]·6H<sub>2</sub>O·2EtOH, and reported an AFM PTMCM–Cu<sup>II</sup> interaction with a  $J/k_{\text{B}}$  value of  $-23.1$  K ( $H = -2J \sum S_{\text{Cu}} S_{\text{radical}}$ ).<sup>4a</sup> The PTM–metal exchange interactions mediated through CO<sub>2</sub><sup>−</sup> groups were also AFM in related complexes.<sup>4b–e</sup> A SO<sub>3</sub><sup>−</sup>-appended PTM, PTMSO<sub>3</sub> (Chart 1), coordinated to a Cu<sup>II</sup> ion to afford [Cu<sup>II</sup>(cyclam)](PTMSO<sub>3</sub>)<sub>2</sub> (cyclam = 1,4,8,11-tetraazacyclotetradecane).<sup>5</sup> The complex exhibited an intramolecular AFM PTMSO<sub>3</sub>–Cu<sup>II</sup> interaction

Chart 1. Chemical Structures of Molecules



with  $J/k_{\text{B}} = -2.3$  K. The magnetic mediations in PTM–metal complexes are mostly AFM. Although some complexes have displayed FM interactions, the mechanism is not fully understood.<sup>6</sup> A new approach for achieving promising FM mediation is necessary to expand the utility of the radicals; the combination of FM and AFM exchange pathways would provide complex magnetic systems with great diversity. The aim of this study is to develop a new method for achieving a definite FM metal–radical exchange coupling in metal complexes coordinated with this class of radical.

We recently prepared a luminescent organic radical, (3,5-dichloro-4-pyridyl)bis(2,4,6-trichlorophenyl)methyl radical (PyBTM), which has a nitrogen atom within the PTM skeleton (Chart 1).<sup>7a</sup> The nitrogen atom is capable of coordinating to metal ions.<sup>7b</sup> Our electron spin resonance (ESR) spectroscopic results and density functional theory (DFT) calculations have shown that the singly occupied molecular orbital (SOMO) is distributed on the  $p\pi$  orbital of the nitrogen atom. Therefore, an efficient PyBTM–metal exchange interaction mediated by the nitrogen atom is expected in PyBTM-ligated complexes; the interaction would be greater than that mediated by CO<sub>2</sub><sup>−</sup> or SO<sub>3</sub><sup>−</sup> linkers. The correct choice of the metal ion (e.g., Cu<sup>II</sup> with a spin on the orbital with  $\sigma$ -bonding nature) is expected to achieve a FM PyBTM–metal interaction because of the orbital orthogonality.

We report herein a novel Cu<sup>II</sup> complex with coordinated PyBTM ligands, Cu<sup>II</sup>(hfac)<sub>2</sub>(PyBTM)<sub>2</sub> (hfac = hexafluoroacetylacetonato; Chart 1). An isostructural Zn<sup>II</sup> complex, Zn<sup>II</sup>(hfac)<sub>2</sub>(PyBTM)<sub>2</sub>, was prepared as a reference. The Cu<sup>II</sup> complex showed a FM exchange interaction between the PyBTM radical and Cu<sup>II</sup> ion with  $J/k_{\text{B}} = 47$  K.

Details of the synthesis and characterization of the complexes are described in the Supporting Information (SI). Single-crystal X-ray diffraction studies revealed that the two M-(hfac)<sub>2</sub>(PyBTM)<sub>2</sub> (M = Cu<sup>II</sup> and Zn<sup>II</sup>) crystals are isostructural with each other. Each unit cell contains two crystallographically

Received: March 3, 2015

Published: April 17, 2015

independent  $M(\text{hfac})_2(\text{PyBTM})_2$  molecules, with the two structures nearly identical. One of the molecular structures of  $\text{Cu}^{\text{II}}(\text{hfac})_2(\text{PyBTM})_2$  is shown in Figure 1a. The  $\text{Cu}^{\text{II}}$  ion is

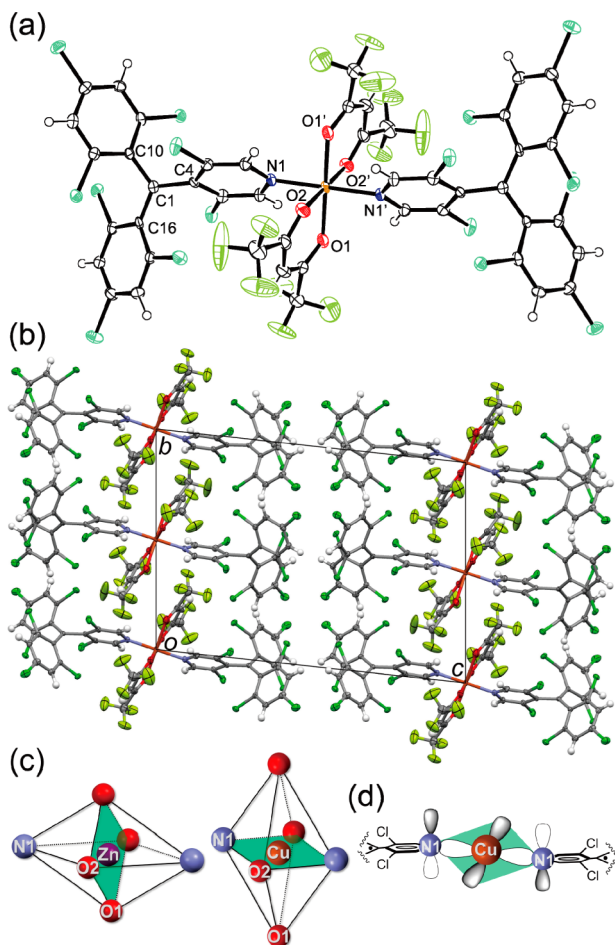


**Figure 1.** Molecular structure of  $\text{Cu}^{\text{II}}(\text{hfac})_2(\text{PyBTM})_2$  (a) and the arrangement viewed along the  $a$  axis in the crystal (b). Schematic representation of the coordination geometry of the complexes (c) and the  $3d_{x^2-y^2}$  orbital of  $\text{Cu}^{\text{II}}$  with the  $\pi$  orbitals at the nitrogen atom in  $\text{PyBTM}$  (d). Disorder of the trifluoromethyl groups is not shown for clarity.

located on an inversion center and forms a distorted octahedral coordination geometry in which two  $\text{PyBTM}$  molecules are coordinated in the trans configuration through the nitrogen atoms. The C1 atom in the  $\text{PyBTM}$  ligands lies in a C4–C10–C16 plane, confirming its  $sp^2$  hybridization. This structural characteristic indicates that the  $\text{PyBTM}$  ligands maintain a radical character. In the  $\text{hfac}$  ligands, one of the two trifluoromethyl groups is disordered in two positions.

Although the two  $M(\text{hfac})_2(\text{PyBTM})_2$  complexes are isostructural, they show differences in the distortion of the coordination geometry around the metal ion. The  $M\text{--O}1$ ,  $M\text{--O}2$ , and  $M\text{--N}$  bond lengths ( $d_{M\text{--O}1}$ ,  $d_{M\text{--O}2}$ , and  $d_{M\text{--N}}$ ), which are the average lengths for the two crystallographically independent complexes, are  $d_{\text{Cu}\text{--O}1} = 2.219$  Å,  $d_{\text{Cu}\text{--O}2} = 2.040$  Å, and  $d_{\text{Cu}\text{--N}} = 2.012$  Å in  $\text{Cu}^{\text{II}}(\text{hfac})_2(\text{PyBTM})_2$  and  $d_{\text{Zn}\text{--O}1} = 2.078$  Å,  $d_{\text{Zn}\text{--O}2} = 2.080$  Å, and  $d_{\text{Zn}\text{--N}} = 2.153$  Å in  $\text{Zn}^{\text{II}}(\text{hfac})_2(\text{PyBTM})_2$ . The octahedral coordination geometry is elongated in the  $\text{Zn}\text{--N}$  direction in the  $\text{Zn}^{\text{II}}$  complex but in the  $\text{Cu}\text{--O}$  direction in the  $\text{Cu}^{\text{II}}$  complex. The  $\text{PyBTM}$  radicals

appear axially coordinated in the  $\text{Zn}^{\text{II}}$  complex and equatorially coordinated in the  $\text{Cu}^{\text{II}}$  complex (Figure 1c).

Such distortion determines the molecular orbital of the  $\text{Cu}^{\text{II}}$  ion on which the unpaired electron exists (i.e., the spin orbital). The  $S = 1/2$  spin on  $\text{Cu}^{\text{II}}$  in  $\text{Cu}^{\text{II}}(\text{hfac})_2(\text{PyBTM})_2$  is expected to be in the  $3d_{x^2-y^2}$ -based orbital; this orbital is distributed along the equatorial  $\text{Cu}\text{--O}2$  and  $\text{Cu}\text{--N}1$  direction and shows  $\sigma$ -bonding character (Figure 1d). Meanwhile, the SOMO (spin orbital) of  $\text{PyBTM}$  on the nitrogen atom has  $p\pi$  character.<sup>7a</sup> In this situation, the two spin orbitals are orthogonal with each other, possibly resulting in a FM interaction.

In the crystal, the two kinds of spin centers ( $\text{Cu}^{\text{II}}$  and C1 atoms) are sterically separated because of the bulkiness of the  $\text{hfac}$  and  $\text{PyBTM}$  moieties (Figure 1b). The shortest intermolecular  $M\text{--M}$  and  $\text{C}1\text{--C}1$  distances are 8.558 and 8.526 Å in  $\text{Cu}^{\text{II}}(\text{hfac})_2(\text{PyBTM})_2$  and 8.550 and 8.596 Å in  $\text{Zn}^{\text{II}}(\text{hfac})_2(\text{PyBTM})_2$ , respectively. Several intermolecular  $\text{Cl}\cdots\text{Cl}$ ,  $\text{Cl}\cdots\text{F}$ ,  $\text{Cl}\cdots\text{H}$ , and  $\text{F}\cdots\text{F}$  atomic contacts are detected that would be responsible for the intermolecular AFM interactions confirmed in the magnetic studies.

The magnetic properties of the complexes were investigated using a SQUID magnetometer. The room-temperature  $\chi T$  value of  $\text{Cu}^{\text{II}}(\text{hfac})_2(\text{PyBTM})_2$  ( $1.21 \text{ cm}^3\cdot\text{K}\cdot\text{mol}^{-1}$ ) was a little higher than that expected from three ideal  $S = 1/2$  spins ( $1.125 \text{ cm}^3\cdot\text{K}\cdot\text{mol}^{-1}$  with  $g = 2.00$ ), confirming the existence of three spins on the complex. The  $\chi T$  value increased upon cooling and reached a maximum at 20 K, indicating a dominant FM interaction between the spins. The subsequent decrease of the  $\chi T$  value below 20 K is attributed to the intermolecular AFM interaction, as discussed for the magnetic properties of  $\text{Zn}^{\text{II}}(\text{hfac})_2(\text{PyBTM})_2$ . The observed FM interaction results from the intramolecular exchange interaction between the  $\text{Cu}^{\text{II}}$  and  $\text{PyBTM}$  spins. The temperature dependence of  $\chi T$  was analyzed by a linear three-spin model with  $H = -J_{\text{Cu}\text{--R}}(S_{\text{Cu}}S_{\text{R}} + S_{\text{R}}S_{\text{Cu}})$ , where  $S_{\text{R}} = S_{\text{Cu}} = 1/2$  and  $J_{\text{Cu}\text{--R}}$  indicates an exchange constant between the spins on  $\text{Cu}^{\text{II}}$  and  $\text{PyBTM}$ .<sup>4a,8</sup> The  $\chi T\text{--}T$  plot was fitted using eq 1 (Figure 2).  $N$ ,  $\mu_{\text{B}}$ , and  $k_{\text{B}}$  indicate the

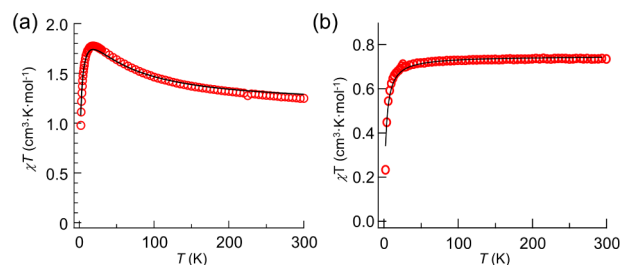


**Figure 2.** Temperature-dependent  $\chi T$  of  $\text{Cu}^{\text{II}}(\text{hfac})_2(\text{PyBTM})_2$  (a) and  $\text{Zn}^{\text{II}}(\text{hfac})_2(\text{PyBTM})_2$  (b) at 1 T. Black lines indicate fitting curves.

Avogadro constant, the Bohr magneton, and the Boltzmann constant, respectively;  $\alpha = J_{\text{Cu}\text{--R}}/T$ , and  $\theta$  represents the intermolecular AFM interactions.<sup>4a,8</sup>

$$\chi T = [N\mu_{\text{B}}^2 g^2 T / 3k_{\text{B}}(T - \theta)] [60 \exp(3\alpha) + 6 \exp(2\alpha) + 6] / [16 \exp(3\alpha) + 8 \exp(2\alpha) + 8] \quad (1)$$

The fitting afforded values for  $J_{\text{Cu}\text{--R}}/k_{\text{B}}$ ,  $g$ , and  $\theta$  of 47 K, 2.05, and  $-1.7$  K, respectively.<sup>9,11</sup> The large positive  $J_{\text{Cu}\text{--R}}/k_{\text{B}}$  value indicates an efficient FM  $\text{PyBTM}\text{--Cu}^{\text{II}}$  interaction that is much stronger than the interaction reported for a  $\text{Cu}^{\text{II}}$  complex with hexacarboxylic radical ligands ( $J_{\text{Cu}\text{--R}}/k_{\text{B}} = 2.1$  K).<sup>6b</sup> This suggests

that the pyridyl group within the triarylphenyl skeleton is superior to the  $\text{CO}_2^-$  group in achieving FM mediation. The origin of the FM coupling can be explained by the nearly orthogonal configuration of the two spin orbitals as discussed in the structural and theoretical studies.

The temperature-dependent  $\chi T$  of  $\text{Zn}^{\text{II}}(\text{hfac})_2(\text{PyBTM})_2$  was analyzed by the Curie–Weiss law to afford a Curie constant ( $C$ ) of  $0.748 \text{ cm}^3 \cdot \text{K} \cdot \text{mol}^{-1}$  and a Weiss constant ( $\theta$ ) of  $-2.4 \text{ K}$  (Figure 2b).<sup>11</sup> The  $C$  value indicates the presence of two PyBTM radicals with the nonmagnetic  $\text{Zn}^{\text{II}}$  ion. The negative  $\theta$  value indicates an AFM interaction between the spin centers. The similarity of the  $\theta$  values of the isostructural  $\text{Cu}^{\text{II}}$  and  $\text{Zn}^{\text{II}}$  complexes confirms the weak intermolecular AFM interaction in the crystals of  $\text{M}(\text{hfac})_2(\text{PyBTM})_2$ .

The intramolecular spin–spin interaction in both complexes could be reproduced by broken-symmetry DFT calculation (Figure 3),<sup>10</sup> in which the geometry of each complex was

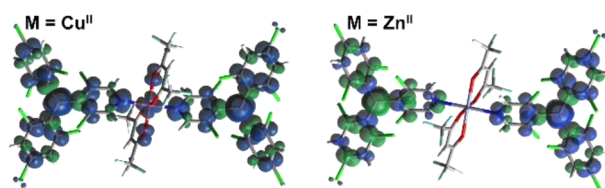


**Figure 3.** Spin-density distribution on  $\text{M}(\text{hfac})_2(\text{PyBTM})_2$  calculated using DFT: uB3LYP/6-31g(d) for C, H, Cl, F, N, and Zn; LANL2DZ for Cu. One of the two crystallographically independent complexes is shown in each complex.

extracted from the crystallographic data.  $\text{Cu}^{\text{II}}(\text{hfac})_2(\text{PyBTM})_2$  demonstrated a quartet ground state. The distribution of the spin density suggests that the spins are located at the  $3d_{x^2-y^2}$ -based orbital on the  $\text{Cu}^{\text{II}}$  ion and the SOMOs on the two PyBTM ligands. The identical sign of the spin density on the centering carbon atoms of the PyBTM ligands and the  $\text{Cu}^{\text{II}}$  ion represents a FM configuration of the spins. Calculated  $J_{\text{Cu-R}}/k_{\text{B}}$  values are 21 and 47 K for the two crystallographically independent molecules and are of the same order as the values obtained experimentally (Table S2 in the SI).  $\text{Zn}^{\text{II}}(\text{hfac})_2(\text{PyBTM})_2$  was calculated to be in the singlet ground state, where intramolecular AFM interactions between the two PyBTM ligands were estimated to be negligible for the two crystallographically independent  $\text{Zn}^{\text{II}}$  complexes ( $J_{\text{R-R}}/k_{\text{B}} = -0.06$  and  $-0.08 \text{ K}$ ). This suggests that the intermolecular AFM coupling would be the dominant factor in the AFM interactions observed in the magnetic studies.

In conclusion,  $\text{Cu}^{\text{II}}(\text{hfac})_2(\text{PyBTM})_2$  and  $\text{Zn}^{\text{II}}(\text{hfac})_2(\text{PyBTM})_2$  were newly prepared. Structural analysis indicated that they had different distortions of the octahedral coordination geometry.  $\text{Cu}^{\text{II}}(\text{hfac})_2(\text{PyBTM})_2$  displayed efficient FM PyBTM– $\text{Cu}^{\text{II}}$  interaction based on the orthogonality of the two spin orbitals.

## ASSOCIATED CONTENT

### Supporting Information

Preparation and characterization of complexes, crystallographic data, parameters calculated using DFT, ESR spectra, absorption and emission spectra, and X-ray crystallographic files in CIF format. This material is available free of charge via the Internet at <http://pubs.acs.org>.

## AUTHOR INFORMATION

### Corresponding Authors

\*E-mail: kusamoto@chem.s.u-tokyo.ac.jp.

\*E-mail: nisihara@chem.s.u-tokyo.ac.jp.

### Notes

The authors declare no competing financial interest.

## ACKNOWLEDGMENTS

The authors thank Dr. Reizo Kato at RIKEN for his kind provision of facilities and laboratory equipment. This work was supported financially by Grants-in-Aid from MEXT of Japan [Grants 24750142, 26220801, and 21108002; area 2107 (coordination programming)].

## REFERENCES

- (1) (a) Hicks, R. G., Ed. *Stable Radicals: Fundamentals and Applied Aspects of Odd-Electron Compounds*; John Wiley & Sons Ltd.: New York, 2010. (b) Caneschi, A.; Gatteschi, D.; Lalioti, N.; Sangregorio, C.; Sessoli, R.; Venturi, G.; Vindigni, A.; Rettori, A.; Pini, M. G.; Novak, M. A. *Angew. Chem., Int. Ed.* **2001**, *40*, 1760–1763. (c) Fedin, M.; Ovcharenko, V.; Sagdeev, R.; Reijerse, E.; Lubitz, W.; Bagryanskaya, E. *Angew. Chem., Int. Ed.* **2008**, *47*, 6897–6899. (d) Miyasaka, H.; Motokawa, N.; Chiyo, T.; Takemura, M.; Yamashita, M.; Sagayama, H.; Arima, T. *J. Am. Chem. Soc.* **2011**, *133*, 5338–5345.
- (2) For example, see: (a) Iwamura, H.; Inoue, K. In *Magnetism: Molecules to Materials II*; Miller, J. S., Drillon, M., Eds.; Wiley-VCH: Weinheim, Germany, 2001; pp 61–108. (b) Rey, P.; Ovcharenko, V. I. In *Magnetism: Molecules to Materials IV*; Miller, J. S., Drillon, M., Eds.; Wiley-VCH: Weinheim, Germany, 2001; pp 41–63.
- (3) (a) Simão, C.; Mas-Torrent, M.; Crivillers, N.; Lloveras, V.; Artés, J. M.; Gorostiza, P.; Veciana, J.; Rovira, C. *Nat. Chem.* **2011**, *3*, 359–364. (b) Ratera, I.; Veciana, J. *Chem. Soc. Rev.* **2012**, *41*, 303–349.
- (4) (a) Maspoch, D.; Ruiz-Molina, D.; Wurst, K.; Vidal-Gancedo, J.; Rovira, C.; Veciana, J. *Dalton Trans.* **2004**, 1073–1082. (b) Maspoch, D.; Gómez-Segura, J.; Domingo, N.; Ruiz-Molina, D.; Wurst, K.; Rovira, C.; Tejada, J.; Veciana, J. *Inorg. Chem.* **2005**, *44*, 6936–6938. (c) Roques, N.; Domingo, N.; Maspoch, D.; Wurst, K.; Rovira, C.; Tejada, J.; Ruiz-Molina, D.; Veciana, J. *Inorg. Chem.* **2010**, *49*, 3482–3488. (d) Maspoch, D.; Domingo, N.; Ruiz-Molina, D.; Wurst, K.; Hernández, J. M.; Lloret, F.; Tejada, J.; Rovira, C.; Veciana, J. *Inorg. Chem.* **2007**, *46*, 1627–1633. (e) Maspoch, D.; Ruiz-Molina, D.; Wurst, K.; Domingo, N.; Cavallini, M.; Biscarini, F.; Tejada, J.; Rovira, C.; Veciana, J. *Nat. Mater.* **2003**, *2*, 190–195.
- (5) Ribas, X.; Maspoch, D.; Wurst, K.; Veciana, J.; Rovira, C. *Inorg. Chem.* **2006**, *45*, 5383–5392.
- (6) (a) Datcu, A.; Roques, N.; Jubera, V.; Maspoch, D.; Fontrodona, X.; Wurst, K.; Imaz, I.; Mouchaham, G.; Sutter, J.; Rovira, C. *Chem.—Eur. J.* **2012**, *18*, 152–162. (b) Roques, N.; Maspoch, D.; Luis, F.; Camón, A.; Wurst, K.; Datcu, A.; Rovira, C.; Ruiz-Molina, D.; Veciana, J. *J. Mater. Chem.* **2008**, *18*, 98–108. (c) Maspoch, D.; Domingo, N.; Ruiz-Molina, D.; Wurst, K.; Hernández, J.-M.; Vaughan, G.; Rovira, C.; Lloret, F.; Tejada, J.; Veciana, J. *Chem. Commun.* **2005**, 5035–5037.
- (7) (a) Hattori, Y.; Kusamoto, T.; Nishihara, H. *Angew. Chem., Int. Ed.* **2014**, *53*, 11845–11848. (b) Hattori, Y.; Kusamoto, T.; Nishihara, H. *Angew. Chem., Int. Ed.* **2015**, *54*, 3731–3734.
- (8) Ishimaru, Y.; Kitano, M.; Kumada, H.; Koga, N.; Iwamura, H. *Inorg. Chem.* **1998**, *37*, 2273–2280.
- (9) The obtained  $g$  value was similar to the value (2.04) estimated from ESR spectroscopy (Figure S1 in the SI).
- (10) (a) Yamaguchi, K.; Kawakami, T.; Takano, Y.; Kitagawa, Y.; Yamashita, Y.; Fujita, H. *Int. J. Quantum Chem.* **2002**, *90*, 370–385. (b) Soda, T.; Kitagawa, Y.; Onishi, T.; Takano, Y.; Shigeta, Y.; Nagao, H.; Yoshioka, Y.; Yamaguchi, K. *Chem. Phys. Lett.* **2000**, *319*, 223–230.
- (11) The  $\theta$  values are converted to intermolecular exchange coupling constants  $zJ/k_{\text{B}}$  of  $-6.8$  and  $-9.6 \text{ K}$  for the  $\text{Cu}^{\text{II}}$  and  $\text{Zn}^{\text{II}}$  complexes, respectively, according to the relation of  $\theta = zJS(S + 1)/3k_{\text{B}}$  with  $S = 1/2$ ; Kahn, O. *Molecular Magnetism*; VCH: New York, 1993.